# On the role of hydronium ions in the protonated micellar aggregates of bile salts

Sofia Candeloro De Sanctis,[a] Angelo A. D'Archivio,[b] Luciano Galantini,[b] Enrico Gavuzzo[c] and Edoardo Giglio *[a]

[a] *Dipartimento di Chimica, Università di Roma "La Sapienza", P.le A. Moro 5, 00185 Roma, Italy*
[b] *Dipartimento di Chimica, Ingegneria Chimica e Materiali, Università di L'Aquila, 67010 L'Aquila, Italy*
[c] *Istituto di Strutturistica Chimica "Giordano Giacomello" CNR, CP No 10, 00016 Monterotondo Stazione, Roma, Italy*

In previous work, structural units observed in bile salt crystals and fibres have been successfully used to represent bile salt micellar aggregates in aqueous solutions and electromotive force measurements have shown that protonated micellar species are present below some critical values of pH. This paper deals with the crystal structures of 3α,12α-dihydroxy-5β-cholanoylglycine (HGDC), 3α,12α-dihydroxy-5β-cholanoyltaurine (HTDC) and 3α,7β-dihydroxy-5β-cholanoyltaurine (HTUDC), which were solved to obtain models of protonated micellar aggregates. The models are compared with those found in crystals and fibres of sodium and rubidium salts of HGDC and HTDC (NaGDC, NaTDC, RbGDC, RbTDC) in order to verify whether the acid structures match with the salt structures. The HGDC packing resembles that of a NaTDC crystal and is stabilized mainly by hydrogen bonds as well as by dipole–dipole interactions between acetone molecules and carboxylic groups. Three different $3_1$ helices are identified. One of these can be easily transformed into the 7/1 helix which satisfactorily describes the NaGDC, NaTDC, RbGDC and RbTDC micellar aggregates. The HTDC and HTUDC crystal structures are practically the same. Strong hydrogen bonds between $H_3O^+$ (hydronium ion) and three oxygen atoms of the anions show O···O distances within the range 2.4–2.6 Å, owing to additional ion–ion and ion–dipole interactions. Very probably, $H_3O^+$ replaces $Na^+$ in the micellar aggregates without remarkably changing their structure because the $H_3O^+$···O and $Na^+$···O distances are very close. Inspection of previous electromotive force data indicates that the glycodeoxycholate and taurodeoxycholate micellar aggregates' proton affinities increase as their sizes increase and that those of the bigger aggregates seem to converge, even though the proton affinity of $COO^-$ is greater than that of $SO_3^-$. These findings strongly suggest that micellization induces $H_3O^+$ binding. HTDC and HTUDC form micellar aggregates which increase their apparent hydrodynamic radius by adding HCl.

## Introduction

Bile acid salts, which play an important role in the biliary and hepatic milieu because of their detergent-like properties, form micellar aggregates in aqueous solutions capable of solubilizing many important biological compounds, for example, cholesterol, phospholipids, bilirubin-IXα and fatty acids. Some are used as drugs for gallstones dissolution. Knowledge of a bile salt micellar structure is crucial for understanding its physicochemical and biological properties. We tackled this problem by using the solid state as a source of models, because equal or similar structures may be present both in the solid and liquid state as frequently occurs for macromolecular compounds.

Sodium salts of 3α,12α-dihydroxy-5β-cholan-24-oic acid (NaDC), 3α,7α-dihydroxy-5β-cholan-24-oic acid, 3α,12α-dihydroxy-5β-cholanoylglycine (NaGDC), 3α,12α-dihydroxy-5β-cholanoyltaurine (NaTDC), 3α,7α,12α-trihydroxy-5β-cholanoylglycine (NaGC), and 3α,7α,12α-trihydroxy-5β-cholanoyltaurine (NaTC) have been investigated together with some rubidium and calcium salts (the Na prefix is replaced with Rb or Ca). In general, the size of the micellar aggregates depends on the ionic strength, pH, temperature, and concentration.[1] Often, the phase transitions: [aqueous micellar solution]→ [gel]→[fiber]→[crystal] are observed by varying the above mentioned parameters. Glassy and birefringent fibres, which sometimes transform into crystals on aging, have been drawn from aqueous micellar solutions near the gelation point and have been studied by X-ray diffraction analysis.[2] The crystal structures of several bile acid salts have been solved.[2d,3] The validity of some models observed in fibres and crystals has been verified by studying aqueous solutions of the micellar aggregates and of their interaction complexes with probe molecules such as bilirubin-IXα, aliphatic and aromatic hydrocarbons, polypeptides, and a spin-labeled cholestane. Small-angle X-ray scattering, electromotive force, extended X-ray absorption fine structure, CD, quasi-elastic light-scattering (QELS), NMR, EPR and dielectric measurements together with energy calculations have been accomplished.[2c–i,3c,f–h,4]

The dihydroxy salt micellar structures of NaDC and RbDC or NaGDC, NaTDC, RbGDC, RbTDC and CaTDC are satisfactorily represented by an 8/1[2h] or 7/1[2e,f] helix, respectively, and the repetitive unit of both helices is a trimer. Moreover, the trihydroxy salt micellar structure of NaTC is in agreement with that of a structural unit formed by dimers, containing a twofold rotation axis or a twofold screw axis.[2i]

Previous electromotive force (emf) measurements of galvanic cells, containing electrodes reversible to $H^+$, $Na^+$ and bile salt anions, carried out on bile salt aqueous solutions as a function of pH, ionic strength and bile salt concentration, provide information on the composition of the micellar aggregates for some bile salts[2i,4e,i,l] and strongly validate the above mentioned models, because the micellar aggregation numbers of NaTDC

**Table 1** Crystallographic data

| Compound | HGDC | HTDC | HTUDC |
|---|---|---|---|
| Formula | $C_{26}H_{43}NO_5 + C_3H_6O$ | $C_{26}H_{45}NO_6S + 2H_2O$ | $C_{26}H_{45}NO_6S + 2H_2O$ |
| FW | 507.7 | 535.7 | 535.7 |
| Crystal size/mm³ | $0.50 \times 0.15 \times 0.15$ | $0.60 \times 0.22 \times 0.20$ | $0.56 \times 0.24 \times 0.21$ |
| Melting point/K | 398 | 432–433 | 432–433 |
| Crystal system | Trigonal | Monoclinic | Monoclinic |
| Space group | $P3_1$ | $P2_1$ | $P2_1$ |
| $a$/Å | 18.275(2) | 9.965(1) | 9.659(3) |
| $b$/Å | 18.275(2) | 8.132(1) | 8.334(2) |
| $c$/Å | 7.383(1) | 17.301(2) | 17.308(5) |
| $\beta$/° | | 90.90(1) | 91.18(2) |
| $V$/Å³ | 2135.4(4) | 1401.8(4) | 1393.0(8) |
| $Z$ | 3 | 2 | 2 |
| $D_{obs}$/g cm⁻³ | 1.17(1) | 1.27(1) | 1.26(1) |
| $D_{calc}$/g cm⁻³ | 1.18 | 1.27 | 1.28 |
| $\mu$/mm⁻¹ | 0.66 | 1.40 | 0.17 |
| Diffractometer | 4-circle Rigaku AFC5R with 12 kW rotating anode (graphite monochromator) | 4-circle Siemens P3 (graphite monochromator) | 4-circle Siemens P3 (graphite monochromator) |
| Wavelength | CuKα ($\lambda = 1.5418$ Å) | CuKα ($\lambda$ 1.5418 Å) | MoKα ($\lambda$ 0.7107 Å) |
| Scan mode | $\theta$–$2\theta$ | $\theta$–$2\theta$ | $\theta$–$2\theta$ |
| No of reflections used for cell constants and orientation matrix | 25 | 15 | 15 |
| $2\theta$ range/° | 5 ÷ 124 | 5.1 ÷ 139 | 4.2 ÷ 65 |
| Measured reflections | | 2977 | 5377 |
| Unique reflections observed | 1936 ($I > 2\sigma(I)$) | 2581 ($I > 2.5\sigma(I)$) | 2773 ($I > 4\sigma(I)$) |
| Program for structure solution | SIR92 | SIR92 | SIR97 |
| Program for structure refinement | SIR-CAOS | SIR-CAOS | SIR-CAOS |
| $R = \Sigma \|\|F_o\| - \|F_c\|\|/\Sigma \|F_o\|$ | 0.044 | 0.066 | 0.036 |
| $R_w = \Sigma w(\|F_o\| - \|F_c\|)^2/\Sigma w \|F_o\|^2$ with $w = (\sin\theta/\lambda)^2$ | 0.056 | 0.083 | 0.046 |
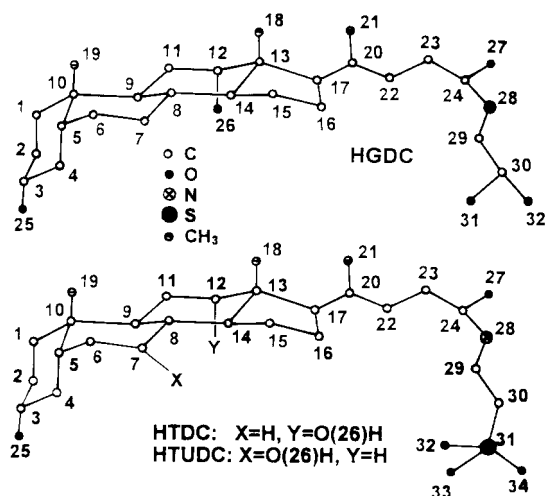


**Fig. 1** Atomic numbering of HGDC, HTDC and HTUDC anions. Hydrogen atoms are omitted.

are mostly multiples of three[2e,4l] and those of NaTC are multiples of two.[2i] In the case of NaDC,[4e] NaGDC,[4i] NaTDC[4l] and NaTC[4n] an increasing protonation of the micellar aggregates occurs when the pH is lowered starting from a critical value. Previous viscosity[2b] and QELS[2h] measurements show that NaDC forms large protonated micellar species as the pH decreases across a narrow range that depends on NaDC concentration, temperature, and ionic strength.

Because H⁺ binds to bile salt micellar aggregates, possible models of the protonated species have been searched for in the crystal structures of 3α,12α-dihydroxy-5β-cholanoylglycine (glycodeoxycholic acid, HGDC), 3α,12α-dihydroxy-5β-cholanoyltaurine (taurodeoxycholic acid, HTDC) and 3α,7β-dihydroxy-5β-cholanoyltaurine (tauroursodeoxycholic acid, HTUDC) (Fig. 1) to establish whether the structures of the acids were similar to those of the salts. The similarity could explain the protonation of the micellar aggregates. Determination of the crystal structures permits a comparison between

the forces which stabilize micellar aggregates containing both bile acid and bile salt molecules.

## Experimental

### Materials

Single crystals of HGDC or HTDC were obtained by adding HCl to an aqueous solution of NaGDC or NaTDC (Sigma) and by slow diffusion of acetone vapours into the solution. HTUDC, kindly supplied by Alpha Wassermann S.p.A., was crystallized from a mixture of water and acetone by diffusion of acetone vapours.

### X-Ray analysis †

Information about data collection, structure solution and refinement procedures is reported in Table 1. X-Ray intensities were collected at room temperature. The scans were carried out at variable and appropriate speeds as a function of the intensity of the reflections. Three standard reflections were monitored during the collection, but negligible decay was observed. The data were corrected for Lorentz and polarisation factors. Owing to the low absorption, no correction was applied to the intensities. The density of the crystals was measured by flotation in a chloroform–chlorobenzene mixture, the density of which was determined by means of a DMA 02C densimeter. The melting points were measured at atmospheric pressure with a Leitz 350 heating plate. Thermogravimetric analyses were accomplished with a Perkin-Elmer Model TGA7 apparatus equipped with a FT-IR Perkin-Elmer 1760X spectrometer. HGDC/acetone, HTDC/$H_2O$, and HTUDC/$H_2O$ ratios of 1, 2, and 2, respectively, were observed.

The structures were solved by direct methods using the program SIR92[5] or SIR97,[6] and refined anisotropically by the full-matrix least-squares method with the program SIR-CAOS.[7] Atomic scattering factors and anomalous dispersion co-
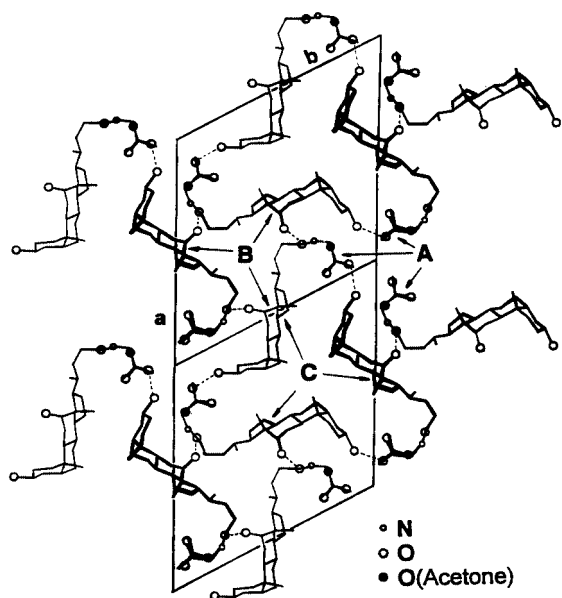
**Fig. 2** HGDC crystal packing viewed along *c*. A thicker line represents an anion nearer to the observer. Broken lines indicate hydrogen bonds. The molecules of the A, B and C $3_1$ helices are indicated by arrows.
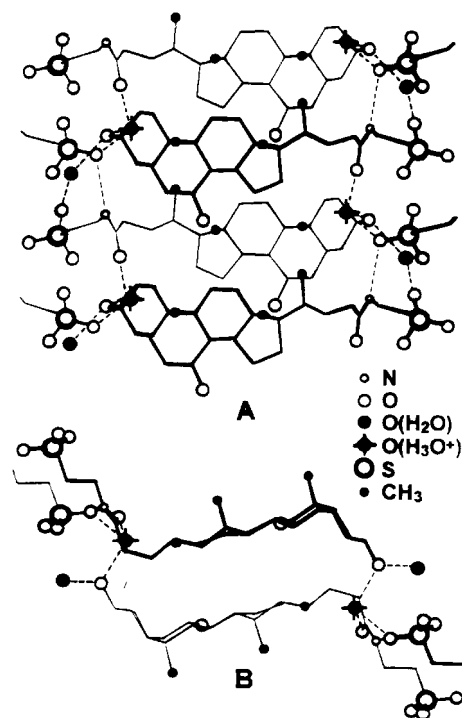


**Fig. 3** HTUDC $2_1$ helix projected (A) along *a*, and (B) along the twofold screw axis. A thicker line represents an anion nearer to the observer. Broken lines indicate hydrogen bonds.

efficients were taken from ref 8. The hydrogen atoms of HGDC and HTDC were generated at the expected positions. Water and hydroxy hydrogens were not taken into account. The H coordinates were not refined and their thermal parameters were set equal to the isotropic ones of the carrier atoms. The hydrogen atoms of HTUDC could be located by means of Fourier syntheses. Their atomic coordinates were refined by using an overall isotropic thermal factor. The bond distances and bond angles were in satisfactory agreement with those usually reported in the literature.

**QELS Measurements**

A Brookhaven instrument constituted of a BI-2030AT digital correlator with 136 channels and a BI-200SM goniometer was used. The light source was an argon ion laser model 85 from Lexel Corporation operating at 514.5 nm. Dust was eliminated by means of a Brookhaven ultrafiltration unit (BIUU1) for flow-through cells, the volume of the flow cell being about 1.0 cm³. Nuclepore filters with a pore size of 0.1 μm were used. The samples were placed in the cell and were allowed to stand 48 hours prior to measurement to obtain reproducible data. Their temperature was kept constant (25 °C) within 0.5 °C by a circulating water bath. The scattered intensity and the time-dependent light scattering correlation function were analysed at a fixed angle of 90°, because they did not vary from 30 to 150°. The scattering decays were analysed by means of cumulant expansion up to second order, because higher order contributions did not improve the statistics. The apparent hydrodynamic radius ($R_h$) was calculated by the Stokes–Einstein relationship.

**Results**

**Crystal structure of HGDC**

The crystal packing (Fig. 2) very closely resembles that of NaTDC.[3b] The HGDC and NaTDC side chains fold back the polar heads and present similar conformations. The crystal packing, as that of NaTDC,[3b] is characterized by $3_1$ helices. Three types of $3_1$ helices (A, B and C) can be identified (Fig. 2). The helices have the outer surface both polar and apolar (A and B) or polar (C). Helices B and C are mainly stabilized by O(26)···O(27) (2.760 Å) and O(25)···O(32) (2.643 Å) hydrogen bonds, respectively. Acetone molecules play an important

role in the growth of the crystal along the *c* axis. They are sandwiched between two carboxylic groups related by a *c* translation. The angle between the least squares plane of the acetone molecule (non hydrogen atoms) and that of the carboxylic group is about 19°. The acetone molecule and the carboxylic group have antiparallel electric dipole moments (the carbonyl bond overlaps the C(29)–C(30) bond in the *ab* projection) and, therefore, the structure is stabilized by dipole–dipole interactions. Moreover, the oxygen atom of the acetone molecule forms a hydrogen bond with O(25) (2.760 Å).

**Crystal structures of HTDC and HTUDC**

HTDC and HTUDC have the same molecular formula and very similar molecular structures (see Fig. 1). Their crystal structures are nearly equal and, therefore, the results are presented and discussed together. Because HTUDC has estimated standard deviations of the atomic parameters and agreement factors $R$ and $R_w$ that are better than HTDC, reference will be made primarily to the HTUDC data. HTDC data are reported in parentheses.

Their crystal packings differ only in the location of the O(26) hydroxy group, which is not involved in strong interactions. A structural unit formed by dimers with a twofold screw axis ($2_1$ helix) is recognizable (Fig. 3). It has a roughly ellipsoidal cross section and an outer surface which is polar near the semimajor axis and nonpolar elsewhere. A water molecule forms two hydrogen bonds with O(25) and O(33) (donor–acceptor distances of 2.644 (2.654) and 2.811 (2.830) Å, respectively). A further N(28)···O(32) hydrogen bond (donor–acceptor distance of 2.856 (2.815) Å) favours the growth of the crystal along *c*. A hydronium ion (H₃O⁺) is located near the polar outer surface (Fig. 3). Its geometry (Fig. 4) indicates that the H₃O⁺ configuration is pyramidal (the distance of the oxygen from the plane of the hydrogens is 0.37 Å), close to tetrahedral.

The HTDC and HTUDC side chain conformations differ from those observed so far. They add to those of NaGDC, CaGDC, NaTDC, RbTDC, NaGC, RbGC, NaTC and RbTC, observed in many crystal structures,[2d,3b–h] and, therefore, the number of the known side chain conformations of the bile salts
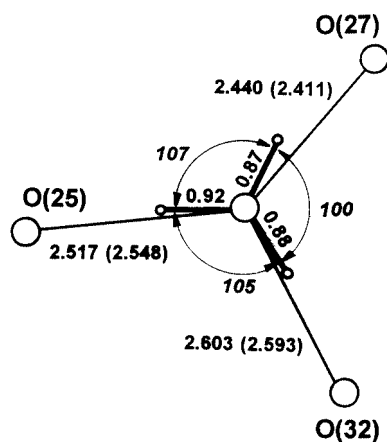
**Fig. 4** Hydrogen bonds and geometry of $H_3O^+$ in the HTUDC crystal. Distances in Å and angles in degrees. The values in parentheses refer to HTDC.
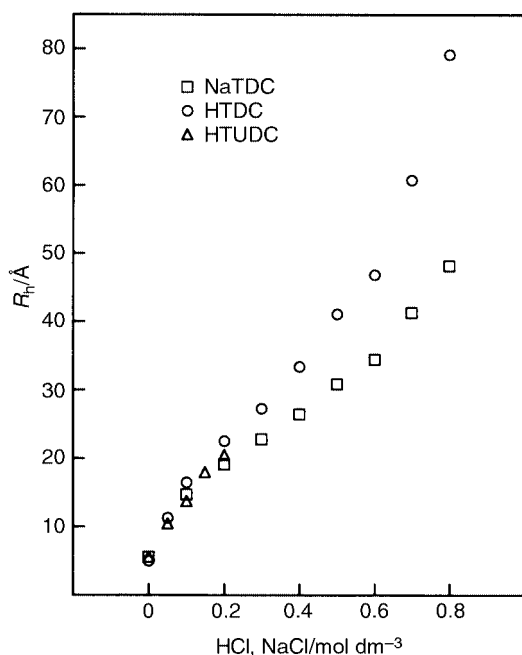


**Fig. 5** $R_h$ as a function of the NaCl or HCl molar concentration for 50 mM aqueous solutions of NaTDC or HTDC and HTUDC. The average standard deviation is ±0.3 Å.

increases. The high side chain conformational flexibility permits satisfying packing and energy requirements through polar interactions.

### QELS Measurements of HTDC and HTUDC aqueous solutions

The progressive protonation of the NaTDC micellar aggregates with decreasing pH[4l] suggests that HTDC could also form micellar aggregates. QELS measurements of HTDC and HTUDC aqueous solutions, containing HCl in order to increase the ionic strength without introducing Na+ ions, give the $R_h$ values shown in Fig. 5 (HTUDC precipitates when the HCl concentration is greater than 0.2 M). Previous data of NaTDC aqueous solutions containing NaCl[2e] are reported for comparison.

## Discussion

7/1 Helices, constituted by trimers, successfully represent the micellar structures of NaGDC, NaTDC, RbGDC, RbTDC and CaTDC.[2e,f] The trimers observed in the helices A, B and C of HGDC differ from those of the 7/1 helices. Helix A, which is stabilized by strong polar interactions in NaTDC, presents

HGDC molecules linked only by weak van der Waals interactions. However, the carboxylic groups could approach the helical axis in water, thus forming hydrogen bonds among them and, probably, with water molecules. Moreover, the helix A trimer has a threefold screw axis whereas the 7/1 helix trimer has a threefold rotation axis. However, the trimer of the helix A can be easily transformed into that of the 7/1 helix by movements like those that a trimer of a RbDC crystal[3a] must undergo to obtain the trimer of the 8/1 helix.[2h] Therefore, the helix A could be a model that, suitably modified, represents the protonated and unprotonated micellar aggregates of NaGDC and NaTDC. On the contrary, helices B and C (see Fig. 2) cannot be easily changed into the 7/1 helix [see Fig. 3 of reference 2(e)].

The $2_1$ helices of HTDC (and HTUDC) cannot be matched with the 7/1 helix of NaTDC. However, the presence of the hydronium ions in the protonated micellar aggregates suggests a reasonable interpretation. The $2_1$ helices, together with structural units containing a twofold rotation axis, have been observed in crystals of RbTDC, CaGDC, NaTC, RbTC, NaGC, and RbGC.[2d,3d–h] The Na+, Rb+ and Ca++ ions are located near the polar outer surface like $H_3O^+$ in the HTDC and HTUDC crystal structures. Therefore, $H_3O^+$ seems to function in the same way as these cations and to be interchangeable with Na+. $H_3O^+$ gives rise to three short O···O distances due to hydrogen bonds reinforced by ion–ion and ion–dipole interactions (Fig. 4). These distances are within the range 2.4–2.6 Å, where most Na+···O contacts lie (see references 3(b)–(f) for NaGDC, NaTDC, NaGC, and NaTC). Hence, the Na+ ions can be replaced by $H_3O^+$ ions as far as the internal energy is concerned ($H_3O^+$ gives rise to additional hydrogen bonds) utilizing the side chain conformational flexibility and without remarkably changing the structure of the micellar aggregates containing Na+ ions only. Reasonably, a similar situation can be hypothesized for the 7/1 and 8/1 helices, which have the cations near the polar heads located in the interior of the helices.[2e,h]

The easy replacement of Na+ with $H_3O^+$ provides an interesting interpretation of some results of the above mentioned emf measurements carried out in the pH range 7–10.[4i,l] They have revealed that the protonation of the NaGDC[4i] and NaTDC[4l] micellar species begins at about the same pH (~8.3), although HGDC and HTDC are a weak and strong acid, respectively. This pH value is too high for NaTDC in comparison with the value of ~5.7 observed for NaTC,[4n] because the acidity of taurocholic acid is comparable to that of HTDC. The proton affinity of the glycodeoxycholate and taurodeoxycholate micellar aggregates (their protonation begins at high pH, about 8.3) is higher than that of the single anions.[4i,l] This strongly suggests that micellization induces $H_3O^+$ binding. The taurodeoxycholate small aggregates are not protonated at variance with the big ones,[4l] whereas some glycodeoxycholate small aggregates (for instance, the dimer) are protonated in all the investigated samples.[4i] Therefore, the glycodeoxycholate micellar aggregate increases the proton affinity by increasing its micellar size less than the taurodeoxycholate micellar aggregate. One possible reason for the convergence of their proton affinities is the decreasing of the monomers and small aggregates percentage by increasing the micellar size. Of course, the proton affinity of the aggregates depends also on their structure. The 7/1 or 8/1 helix, proposed for NaGDC and NaTDC or NaDC micellar aggregates, respectively, is able to accommodate the hydronium ions. The location of the Na+ ions (and, hence, of the $H_3O^+$ ions) is near the COO− and $SO_3^-$ groups, which are in the interior of the helices, as can be inferred from potential energy calculations[2e,h] and crystal structures.[3b,c] Since $H_3O^+$ forms strong interactions with the anions in these similar helical structures, the high proton affinity of the taurodeoxycholate and glycodeoxycholate anions in the micellar aggregates is accounted for.

On the basis of the easy protonation of the NaTDC micellar

aggregates by adding a very small amount of HCl,[4l] the free energy gain associated with the transfer of $H_3O^+$ from the bulk solution to the micellar aggregate should be greater than in the case of $Na^+$. For this reason and because of the high solubility in water of HTDC, the complete protonation of the NaTDC micellar aggregates by lowering the pH was considered possible. In this case, HTDC micellar aggregates should be present. QELS measurements of HTDC and HTUDC aqueous solutions containing HCl were carried out to verify this hypothesis. The HTDC and HTUDC $R_h$ values can be compared with previous data of NaTDC aqueous solutions containing NaCl[2e] (Fig. 5). The $R_h$ values of HTDC, greater than those of NaTDC, increase with the HCl concentration and suggest that the HTDC micellar size is greater than that of NaTDC as well as that the $H_3O^+$ ions have a higher affinity than the $Na^+$ ions for the taurodeoxycholate micellar aggregates. HTUDC behaves as HTDC up to a HCl concentration 0.2 M.

A last point deserves some attention. NaDC aggregates, represented by 8/1 helices, have been protonated by adding a small amount of HCl ($[Na^+]/[H_3O^+] \approx 10$) up to almost the gelation point, where fibres, formed by 8/1 helices containing $Na^+$ and, to a less extent, $H_3O^+$ ions, have been drawn.[2h] A little lowering of pH or temperature caused the formation of a gel characterized by a bimodal $R_h$ distribution, corresponding to very small and very big aggregates.[2h] The absence of an appreciable rotational contribution in the mechanism causing the decay of the intensity autocorrelation function has been ascribed to the presence of roughly isotropic big aggregates with spheroidal shape. Because the gel formation depends on the decrease of pH, it has been proposed that a possible model of the big aggregate could be a set of 8/1 helices with their helical axes irradiating towards a spherical surface from a center constituted by a solvated hydrogen ion or a cluster containing hydrogen ions and water molecules.[2h] Plainly, protonation of the NaDC micellar aggregates by adding HCl up to the gelation point reasonably takes place[4e] as in the case of NaGDC and NaTDC, because the structures of the 8/1 and 7/1 helices are similar. On the other hand, an uptake of $H^+$ has been observed during the gel formation (obtained by adding HCl and/or NaCl),[9a,b] accompanied by negative changes of volume, entropy, and enthalpy.[9c] Therefore, because the polar interactions (*i.e.*, ion–ion, ion–dipole, and hydrogen bonding) generally cause negative changes of volume and enthalpy and the apolar ones (*i.e.*, hydrophobic interactions) cause positive changes of volume and entropy, the formation of hydrogen bonds has been invoked.[9a,b] Moreover, earlier measurements of the $H^+$ and $Na^+$ activity change with concentration[9a,d] have led to the conclusion that $H^+$ ions replace $Na^+$ ions during the gel formation and produce a more stable structure by means of hydrogen bonding. All these results agree with the presence and the properties of $H_3O^+$ (which gives rise to ion–ion and ion–dipole interactions as well as to hydrogen bonds) and water clusters $(H_2O)_nH_3O^+$.

## Acknowledgements

## References

1 M. C. Carey, *Sterols and Bile Acids*, eds. H. Danielsson and J. Sjøvall, Elsevier/North-Holland Biomedical Press, Amsterdam, 1985, p. 345.
2 (*a*) A. Rich and D. M. Blow, *Nature* (*London*), 1958, **182**, 423; (*b*) D. M. Blow and A. Rich, *J. Am. Chem. Soc.*, 1960, **82**, 3566; (*c*) G. Conte, R. Di Blasi, E. Giglio, A. Parretta and N. V. Pavel, *J. Phys. Chem.*, 1984, **88**, 5720; (*d*) M. D'Alagni, A. A. D'Archivio, E. Giglio and L. Scaramuzza, *J. Phys. Chem.*, 1994, **98**, 343; (*e*) G. Briganti, A. A. D'Archivio, L. Galantini and E. Giglio, *Langmuir*, 1996, **12**, 1180; (*f*) A. A. D'Archivio, L. Galantini and E. Giglio, *Langmuir*, 1997, **13**, 4197; (*g*) M. D'Alagni, A. A. D'Archivio, L. Galantini and E. Giglio, *Langmuir*, 1997, **13**, 5811; (*h*) A. A. D'Archivio, L. Galantini, E. Giglio and A. Jover, *Langmuir*, 1998, **14**, 4776; (*i*) E. Bottari, A. A. D'Archivio, M. R. Festa, L. Galantini and E. Giglio, *Langmuir*, 1999, **15**, 2996.
3 (*a*) A. R. Campanelli, S. Candeloro De Sanctis, E. Giglio and S. Petriconi, *Acta Crystallogr.*, *Sect. C*, 1984, **40**, 631; (*b*) A. R. Campanelli, S. Candeloro De Sanctis, E. Giglio and L. Scaramuzza, *J. Lipid Res.*, 1987, **28**, 483; (*c*) A. R. Campanelli, S. Candeloro De Sanctis, E. Chiessi, M. D'Alagni, E. Giglio and L. Scaramuzza, *J. Phys. Chem.*, 1989, **93**, 1536; (*d*) A. R. Campanelli, S. Candeloro De Sanctis, L. Galantini and E. Giglio, *J. Inclusion Phenom. Mol. Recognit. Chem.*, 1991, **10**, 367; (*e*) A. R. Campanelli, S. Candeloro De Sanctis, A. A. D'Archivio and E. Giglio, *J. Inclusion Phenom. Mol. Recognit. Chem.*, 1991, **11**, 247; (*f*) M. D'Alagni, L. Galantini, E. Giglio, E. Gavuzzo and L. Scaramuzza, *J. Chem. Soc.*, *Faraday Trans.*, 1994, **90**, 1523; (*g*) A. A. D'Archivio, L. Galantini, E. Gavuzzo, E. Giglio and L. Scaramuzza, *Langmuir*, 1996, **12**, 4660; (*h*) A. A. D'Archivio, L. Galantini, E. Gavuzzo, E. Giglio and F. Mazza, *Langmuir*, 1997, **12**, 3090.
4 (*a*) M. D'Alagni, M. L. Forcellese and E. Giglio, *Colloid Polym. Sci.*, 1985, **263**, 160; (*b*) G. Esposito, E. Giglio, N. V. Pavel and A. Zanobi, *J. Phys. Chem.*, 1987, **91**, 356; (*c*) G. Esposito, A. Zanobi, E. Giglio, N. V. Pavel and I. D. Campbell, *J. Phys. Chem.*, 1987, **91**, 83; (*d*) E. Giglio, S. Loreti and N. V. Pavel, *J. Phys. Chem.*, 1988, **92**, 2858; (*e*) E. Bottari, M. R. Festa and R. Jasionowska, *J. Inclusion Phenom. Mol. Recognit. Chem.*, 1989, **7**, 443; (*f*) E. Chiessi, M. D'Alagni, G. Esposito and E. Giglio, *J. Inclusion Phenom. Mol. Recognit. Chem.*, 1991, **10**, 453; (*g*) E. Burattini, P. D'Angelo, E. Giglio and N. V. Pavel, *J. Phys. Chem.*, 1991, **95**, 7880; (*h*) M. D'Alagni, M. Delfini, L. Galantini and E. Giglio, *J. Phys. Chem.*, 1992, **96**, 10520; (*i*) E. Bottari and M. R. Festa, *Monatsh. Chem.*, 1993, **124**, 1119; (*j*) M. D'Alagni, A. A. D'Archivio and E. Giglio, *Biopolymers*, 1993, **33**, 1553; (*k*) P. D'Angelo, A. Di Nola, E. Giglio, M. Mangoni and N. V. Pavel, *J. Phys. Chem.*, 1995, **99**, 5471; (*l*) E. Bottari and M. R. Festa, *Langmuir*, 1996, **12**, 1777; (*m*) A. Bonincontro, G. Briganti, A. A. D'Archivio, L. Galantini and E. Giglio, *J. Phys. Chem.*, 1997, **101**, 10303; (*n*) E. Bottari, M. R. Festa and M. Franco, *Analyst*, 1999, **124**, 887.
5 A. Altomare, G. Cascarano, C. Giacovazzo, A. Guagliardi, M. C. Burla, G. Polidori and M. Camalli, *J. Appl. Crystallogr.*, 1994, **27**, 435.
6 G. Cascarano, A. Altomare, C. Giacovazzo, A. Guagliardi, A. G. G. Moliterni, D. Siliqi, M. C. Burla, G. Polidori and M. Camalli, *Acta Crystallogr.*, *Sect. A*, 1996, **52**, C-79.
7 M. Camalli, D. Capitani, G. Cascarano, S. Cerrini, C. Giacovazzo and R. Spagna, SIR-CAOS. *User Guide*; Istituto di Strutturistica Chimica CNR C. P. no. 10, 00016 Monterotondo Stazione, Roma, 1986.
8 *International Tables for X-ray Crystallography*, Kynoch Press, Birmingham, England, 1974, Vol. IV.
9 (*a*) G. Sugihara, M. Tanaka and R. Matuura, *Bull. Chem. Soc. Jpn.*, 1977, **50**, 2542; (*b*) G. Sugihara, K. Motomura and R. Matuura, *Mem. Fac. Sci. Kyushu Univ.*, *Ser. C*, 1970, **7**, 103; (*c*) G. Sugihara, T. Ueda, S. Kaneshina and M. Tanaka, *Bull. Chem. Soc. Jpn.*, 1977, **50**, 604; (*d*) G. Sugihara and M. Tanaka, *Bull. Chem. Soc. Jpn.*, 1976, **49**, 3457.

*Paper a902558h*